VOL.101 NO.GT2. FEB. 1975

JOURNAL OF THE GEOTECHNICAL ENGINEERING DIVISION

PROCEEDINGS OF
THE AMERICAN SOCIETY
OF CIVIL ENGINEERS

VOL.101 NO.GT2. FEB. 1975

JOURNAL OF THE GEOTECHNICAL ENGINEERING DIVISION

PROCEEDINGS OF
THE AMERICAN SOCIETY
OF CIVIL ENGINEERS

CONTENTS

Heat Transfer in Soil-Water-Ice Systems
by Aditya Mohan 97

Creep of Sand-Ice System
by Robert G. Rein, Jr., Vidyutkumar V. Hathi, and Cedomir M. Sliepcevich 115

Photoelastic Analysis of a Cofferdam
by Naveed K. Burki and Rowland Richards, Jr. 129

Effects of Deforestation on Slopes
by Colin B. Brown and Maw S. Sheu 147

Seismic Design of Reinforced Earth Walls
by Gregory N. Richardson and Kenneth L. Lee 167

Prediction of Downdrag Forces in End-Bearing Piles
by Harry G. Poulos and Edward H. Davis 189

DISCUSSION

Proc. Paper 11087

Settlement of Dry Sands During Earthquakes, by H. Bolton Seed and Marshall L. Silver (Apr., 1972. Prior Discussions: Dec., 1972).
closure 207

→

This Journal is published monthly by the American Society of Civil Engineers. Publications office is at 345 East 47th Street, New York, N.Y. 10017. Address all ASCE correspondence to the Editorial and General Offices at 345 East 47th Street, New York, N.Y. 10017. Allow six weeks for change of address to become effective. Subscription price to members is $10.00. Nonmember subscriptions available; prices obtainable on request. Second-class postage paid at New York, N.Y. and at additional mailing offices. HY, GT.

Finite Element for Rock Joints and Interfaces, by Jamshid Ghaboussi, Edward L. Wilson, and Jeremy Isenberg (Oct., 1973. Prior Discussion: Aug., 1974).
closure 207

The Nature of Lunar Soil, by W. David Carrier, III, James K. Mitchell, and Arshud Mahmood (Oct., 1973).
errata 208

Settlement of Building on Pile Foundation in Sand,[a] by Robert M. Koerner and Antal Partos (Mar., 1974. Prior Discussion: Oct., 1974).
by William D. Kovacs and Gerald A. Leonards 209

Planning and Performing Compaction Grouting,[a] by James Warner and Douglas R. Brown (June, 1974).
by Robert Wade Brown 211

Review of Expansive Soils,[a] by Gerald J. Gromko (June, 1974. Prior Discussion: Jan., 1975).
by Lawrence D. Johnson and Donald R. Snethen 213

TECHNICAL NOTES

Proc. Paper 11093

Lateral Stress in Sands During Cyclic Loading
by T. Leslie Youd and Terry N. Craven 217

Effect of Interface Continuity on Pavement Moments
by Satya P. Keshava and Kulbhushan L. Chhibber 222

[a]Discussion period closed for this paper. Any other discussion received during this discussion period will be published in subsequent Journals.

11123 HEAT TRANSFER IN SOIL-WATER-ICE SYSTEMS

KEY WORDS: Environmental effects; Finite element method; **Frost action; Geotechnical engineering; Heat transfer; Ice;** Permafrost; Soil mechanics; **Soils;** Thermal analysis; **Water**

ABSTRACT: The finite element method has an excellent solution capability for problems requiring transient temperature distribution under time-dependent temperature initial and boundary conditions. Some exceptional features in handling are: space variations of temperature-dependent material properties, irregular boundary geometries of problem regions, temperature and heat flux boundary conditions at any point in the problem region, and freedom in varying the size of the finite discretization within the problem region. This paper presents a general computer-oriented solution technique for geotechnical problems of heat conduction, including the effect of latent heat generation and absorption. A variational principle is applied for initial boundary value problems of unsteady heat flow, and the finite elements method is used to generate approximate solutions to plane and axisymmetric problems. Variation in physical and thermal properties of materials with both temperature and space, and functional relationships between the amount of water frozen and the temperature are taken into account automatically during the process of heat conduction.

REFERENCE: Mohan, Aditya, "Heat Transfer in Soil-Water-Ice Systems," *Journal of the Geotechnical Engineering Division,* ASCE, Vol. 101, No. GT2, **Proc. Paper 11123**, February, 1975, pp. 97-113

11134 CREEP OF SAND-ICE SYSTEM

KEY WORDS: **Creep;** Deformation; **Frozen soils; Geotechnical engineering; Limiting factors;** Sands; Soil mechanics; **Strain rate**

ABSTRACT: Unconfined uniaxial creep tests were conducted at −8.5°C on sand-ice samples with an average wet density of 124 pcf (1,986 kg/m^3). The samples were 94% water saturated, on the average, prior to freezing. Thus the data represent the behavior of slightly undersaturated frozen sands. Stress-strain data for different durations of loading were obtained by replotting the creep data. Values of the stress characterizing the change in stress-strain relations are confirmed by creep rate-stress data. It is shown that use of a single continuous stress function to represent stress-strain data in models must be limited to either stresses greater than, or less than, the limiting long-term strength. A single continuous stress function cannot represent realistically the entire stress range.

REFERENCE: Rein, Robert G., Jr., Hathi, Vidyutkumar V., and Sliepcevich, Cedomir M., "Creep of Sand-Ice System," *Journal of the Geotechnical Engineering Division,* ASCE, Vol. 101, No. GT2, **Proc. Paper 11134**, February, 1975, pp. 115-128

11135 PHOTOELASTIC ANALYSIS OF A COFFERDAM

KEY WORDS: Bearing capacity; **Cofferdams;** Earth pressure; Elasticity; **Failure; Geotechnical engineering; Photoelasticity;** Shear; Sheet piling; **Soil mechanics;** Stresses

ABSTRACT: Elastic stresses inside the soil mass of a cofferdam are determined using photoelastic technique. A cofferdam model was fabricated simulating the soil mass with gelatin and the steel sheet piles with urethane rubber. This model was tested in a state of plain strain, and, from the photoelastic data, elastic stresses within the fill material were found due to both gravity loading and water pressure. In the gravity loading case, normal stresses agree with the standard theory of soil mechanics for geostatic stresses. Water pressure introducing bending is found to affect the stresses appreciably causing a nonlinear distribution of stresses and pressure on the base of the cofferdam. Contrary to many theories, shear stresses are found to be higher near the sheet pile walls than the midplane. New failure surfaces, in accordance with the elastic stress state, are postulated.

REFERENCE: Burki, Naveed K., and Richards, Rowland, Jr., "Photoelastic Analysis of a Cofferdam," *Journal of the Geotechnical Engineering Division,* ASCE, Vol. 101, No. GT2, **Proc. Paper 11135**, February, 1975, pp. 129-145

JOURNAL OF THE GEOTECHNICAL ENGINEERING DIVISION

EFFECTS OF DEFORESTATION ON SLOPES

By Colin B. Brown,[1] M. ASCE and Maw S. Sheu[2]

INTRODUCTION

Gray (10) has recognized four ways in which vegetation affects slopes: (1) The root system provides mechanical reinforcement to the soil; (2) vegetation provides a vertical slope surcharge; (3) wind in the trees causes surface shears and moments; and (4) soil moisture content and water level are modified by vegetation changes.

There are two schools of thought concerning the subsequent slope stability and creep rates after forest tree removal. In reporting soil mantle motions in Queensland after forest clearing, Ellison and Coaldrake (5) claimed that creep rates were higher for slopes covered by trees than for those covered by sod in rain forests. In their view, slope instabilities more readily occur with a heterogeneous forest overburden than with a sod covering. Flaccus (7) in his doctoral dissertation indicated that clear cutting in New England had no part in the occurrence of slides and, in fact, reduced a slope's susceptibility to sliding. On the other hand, evidence in various parts of the world suggests that the deterioration of the root support system that occurs after logging is the main factor in the increase in creep rates and sliding. Bishop and Stevens (2) in Alaska noted that despite higher rainfall in the year before cutting, more slides occurred after deforestation. They ascribed this to the deterioration of the interconnected root system after logging. Croft and Adams (3) in Utah concluded that at Wasatch Mountain the loss of mechanical support by the root system after cutting increased landslide frequency. In Japan, Kawaguchi, et al. (15) found that the occurrence of slides decreased with the age of the forest timber. The highest likelihood of slope instability was in young forest stands, shrublands, and grasslands.

These clear differences in attitudes concerning clear cutting indicate that the

Note.—Discussion open until July 1, 1975. To extend the closing date one month, a written request must be filed with the Editor of Technical Publications, ASCE. This paper is part of the copyrighted Journal of the Geotechnical Engineering Division, Proceedings of the American Society of Civil Engineers, Vol. 101, No. GT2, February, 1975. Manuscript was submitted for review for possible publication on August 21, 1974.

[1]Prof., Dept. of Civ. Engrg., Univ. of Washington, Seattle, Wash.
[2]Grad. Student, Dept. of Civ. Engrg., Univ. of Washington, Seattle, Wash.

effect is not properly understood. By incorporating the work of Ter-Stepanian (19) and Yen (20) on creep, slope stability analyses, and Gray's (10) four features concerning vegetation effects on soil slopes, an analysis is proposed herein that predicts creep rates and instabilities in infinite uniform slopes before and after logging. The results indicate if and when slope instability will occur and the historical creep rate. Thus, a clearer picture of the effect of clear cutting on slopes appears and some of the previously mentioned contentious views are resolved.

The first part of the paper idealizes the ground and then includes the four previously mentioned vegetation effects as mechanical features subject to rigorous analysis. With this completed the analysis for creep and instability follows; finally, examples are considered that lead to practical conclusions.

Ground Idealization

The ground is considered as an infinite soil slope of angle β founded on bedrock. Points in the soil are located by the vertical coordinate, Z, with $Z = 0$ in the soil-bedrock interface. The soil surface is $Z = H$ and the phreatic surface of the ground-water table is $Z = H_W$. For $H_W < Z \leq H$, the soil density is γ and for $0 < Z \leq H_W$ is γ_s, the saturated density (see Fig. 1).

The soil properties are taken as steady, i.e., consolidation and other time-dependent features are completed; inertia effects are ignored. The steady creep rate parallel to the slope, V, has a gradient with respect to the normal to the slope of dV/dN. This gradient is related to the shear stress, τ, by considering the soil as a Bingham substance (14) with linear Newtonian coefficient of viscosity η. Then

$$\frac{dV}{dN} = 0; \quad 0 < \tau \leq \tau_o \quad \ldots\ldots\ldots\ldots\ldots\ldots\ldots\ldots\ldots\ldots\ldots\ldots\ldots\ldots (1a)$$

$$\tau = \tau_o + \eta \frac{dV}{dN}; \quad \tau_o < \tau \leq \tau_u \quad \ldots\ldots\ldots\ldots\ldots\ldots\ldots\ldots\ldots\ldots\ldots\ldots (1b)$$

in which η depends on the effective normal stress, σ'; τ_o separates the rigid phase where Eq. 1*a* applies from the creep phase where Eq. 1*b* applies; and τ_u = the ultimate shear strength.

Root System

The mantle soil without the root system has an ultimate shear capacity, τ_u, described by the Coulomb law:

$$\tau_u = C_u + \sigma' \tan \phi \quad \ldots\ldots\ldots\ldots\ldots\ldots\ldots\ldots\ldots\ldots\ldots\ldots\ldots\ldots (2)$$

in which C_u = the cohesion capacity; σ' = the effective normal compression stress on the shear plane; and ϕ = the angle of internal friction. The separation between the rigid and creep phases given in Eqs. 1 by τ_o is related to the mobilized cohesion, C_o, and the shear angle parameter, θ_o, as

$$\tau_o = C_o + \sigma' \tan \theta_o \quad \ldots\ldots\ldots\ldots\ldots\ldots\ldots\ldots\ldots\ldots\ldots\ldots\ldots\ldots (3)$$

In the manner of Ter-Stepanian (19) the cohesions and shear angles in Eqs.

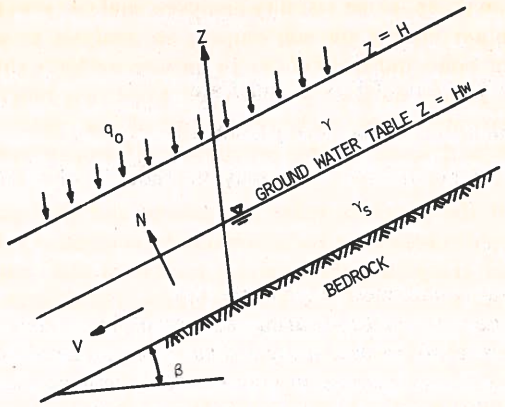

FIG. 1.—Slope Idealization

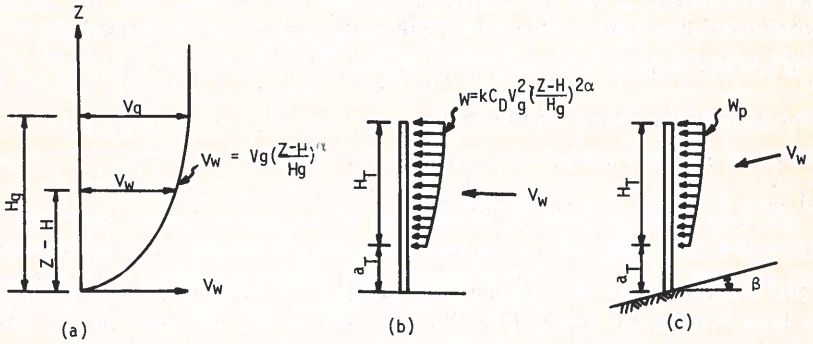

FIG. 2.—Wind Gradient and Pressures

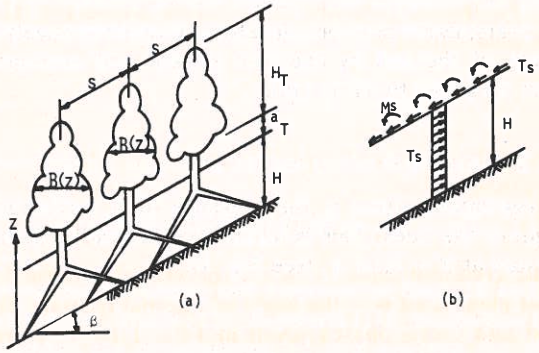

FIG. 3.—Wind Effects on Trees and Mantle

2 and 3 may be utilized to describe the initial tensile strength of the soil, σ_i. Then

$$C_u = \sigma_i \tan \phi; \quad C_o = \sigma_i \tan \theta_o \quad \ldots \quad (4)$$

and the limiting situations of Eqs. 2 and 3 are

$$\tau_u = (\sigma_i + \sigma') \tan \phi; \quad \tau_o = (\sigma_i + \sigma') \tan \theta_o \quad \ldots \quad (5)$$

Other values of shear stress $\tau < \tau_u$ may be thought of in the same manner in which

$$\tau = (\sigma_i + \sigma') \tan \theta \quad \ldots \quad (6)$$

and θ is the partially mobilized shear angle (19).

The effect of tree roots on the shearing capacity of the soil has been investigated by Endo and Tsuruta (6). In that study a shear strength amplification was found to be associated with an increase in cohesion only and no change in the shear angle parameter. This change in cohesion can be reflected by an increase in tensile capacity from σ_i to $(\sigma_i + \sigma_\gamma)$, in which σ_γ is a measure of the effect of the tree root system on the cohesion of the soil. With the limiting shear angle parameters, ϕ and θ_o, indifferent to the root system, then the limiting cohesions of Eqs. 4 in the presence of the root system can be defined as

$$C_u = (\sigma_i + \sigma_\gamma) \tan \phi; \quad C_o = (\sigma_i + \sigma_\gamma) \tan \theta_o \quad \ldots \quad (7)$$

The equations equivalent to Eqs. 5 are

$$\tau_u = (\sigma_i + \sigma_\gamma + \sigma') \tan \phi; \quad \tau_o = (\sigma_i + \sigma_\gamma + \sigma') \tan \theta_o \quad \ldots \quad (8)$$

and for $\tau < \tau_u$, Eq. 6 may be written as

$$\tau = (\sigma_i + \sigma_\gamma + \sigma') \tan \theta \quad \ldots \quad (9)$$

The density of the root system as a function of position in the soil mantle has been studied by Gaiser (9). Thus, σ_γ will depend not only on the time, t, after logging but also on the position in the soil, Z. The time element provides for the deterioration of the root system after logging. Thus

$$\sigma_\gamma = \sigma_\gamma(Z, t) \quad \ldots \quad (10)$$

The previous examination provides, in a form suitable for analytical treatment, the reinforcement of the soil by the root system and accounts for the first vegetation effect proposed by Gray (10).

Tree Surcharge

The second vegetation effect is the presence of a surcharge on the slope due to the weight of the trees. This is taken into account by including a vertical downward pressure at $Z = H$ of q_o (see Fig. 1).

Wind in Trees

In order to determine the effect of wind blowing in forest trees, it is necessary to find expressions that relate wind speeds to pressures. If the local pressure is w, parallel to the wind of speed V_w, then (4)

$$w = k C_D V_w^2 \quad \ldots \quad (11)$$

in which k is a coefficient depending on the units used; and C_D = the drag coefficient.

The wind speed, V_w, occurs in the boundary layer of the earth. The separation between inviscid and viscous flow occurs at a height, H_G, above the local surface. The height, H_G, varies according to whether the area is mountainous or flat, builtup or rural, maritime or inland. The shape of the wind speed profile for heights smaller than H_G is (4)

$$V_w = V_g \left(\frac{Z - H}{H_G} \right)^\alpha \quad \ldots \quad (12)$$

in which the exponent, α, like H_G depends upon local features; and V_g = the air-stream velocity at H_G.

The relation between V_w [shown in Fig. 2(*a*)] and w is therefore

$$w = k C_D V_g^2 \left(\frac{Z - H}{H_G} \right)^{2\alpha} \quad \ldots \quad (13)$$

The wind pressure on the tree is shown in Fig. 2(*b*). Our interest is in the tree on the slope of β where V_w blows down the slope. The pressure normal to the tree is then

$$w_p = \frac{2w \cos \beta}{1 + \cos^2 \beta} \quad \ldots \quad (14)$$

The wind forces transmitted to the ground are now obtained (see Fig. 3). Considering trees spaced S apart down and across the slope with lower limbs starting at a_T above the ground and of total height $(a_T + H_T)$, then the force transmitted by a single tree parallel to the ground is

$$F_S = \int_{H+a_T}^{H+a_T+H_T} B(Z)\, w_p(Z) \cos dZ \quad \ldots \quad (15)$$

in which $B(Z)$ = breadth of the limbed tree between the limits. The shear force per unit area normal to the slope is

$$T_S = \frac{F_S}{S^2} \quad \ldots \quad (16)$$

The bending moment per unit area normal to the slope about $Z = H$ is

$$M_S = \frac{1}{S^2} \int_{H+a_T}^{H+a_T+H_T} B(Z)\, w_p(Z)\, (Z - H)\, dZ \quad \ldots \quad (17)$$

The transmission of the forces and moments in Eqs. 16 and 17 is by virtue of the tree root system. Holch (12), Heyward (11), McQuilkin (16), and Gaiser (9) have investigated the development of root systems for different species and sites. The roots have, in general, radial symmetry about the tree trunk axis and are spread out in such a way that they entangle with roots of other trees in a forest. The density of the system tends to increase from $Z = 0$

to a maximum at about $Z = (H - 2')$. At this stage the root system resistance is considered to be independent of Z.

Soil Moisture Content

This is the last feature raised by Gray (10). Here we consider a phreatic surface at $Z = H_w$ and define

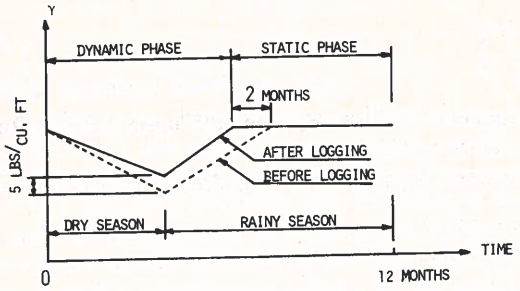

FIG. 4.—Variation of γ with Time

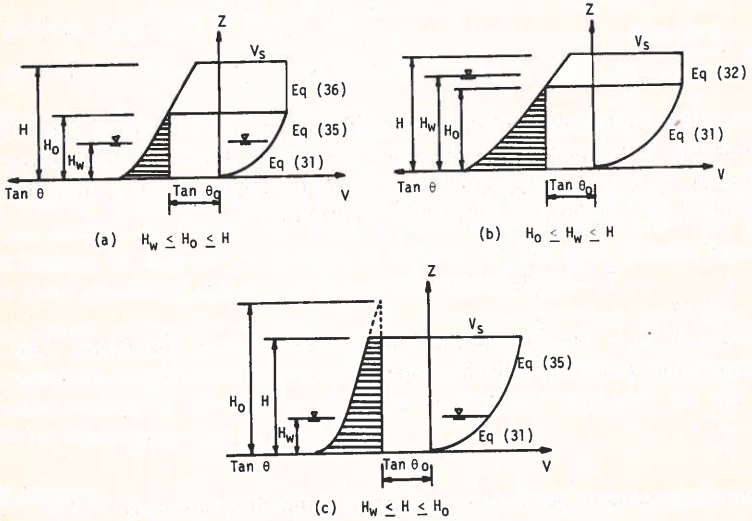

FIG. 5.—Creep Speeds and tan θ as Function of Depth Z

$$H = H_w + H_u \quad \ldots\ldots\ldots\ldots\ldots\ldots\ldots\ldots\ldots\ldots\ldots\ldots \quad (18)$$

The first concern is in the change of moisture content of the soil, $Z > H_w$, after logging. The presence of trees depletes the water and reduces the average unit weight of the soil, γ. This depletion is due to evapotranspiration (14). Bethlahmy (1) divided the year into static and dynamic parts. The static part is the steady water regime of the soil in the rainy season. At the conclusion

of this, the water content is reduced throughout the dry season and then builds up again at the beginning of the rainy season to static conditions. The dynamic part is the dry season and the beginning of the rainy season. These measurements are of importance in this study: (1) The lowest $\gamma = \gamma_1$ (at the end of the dry season); (2) the highest $\gamma = \gamma_2$ (steady part); and (3) the time between 1 and 2 (see Fig. 4).

For 1 it has been found that in the year after logging an increase in γ_1 of about 4 pcf-5 pcf (64 kg/m^3-80 kg/m^3) occurs. The value for 2, γ_2, is unaltered after logging. The time for the steady part to commence is about 2 months longer before logging than after. Beyond the first year after logging, there is a rapid tendency for γ_1 to return to the value in the forested state (11).

The second concern is the change of H_w after logging. The trees not only deplete the water content in $Z > H_w$ but also depress H_w. The absence of evapotranspiration after logging may result in the increase in H_w.

Creep Analysis

This analysis extends the work of Ter-Stepanian (19). Included are the features associated with deforestation previously described. The effect of wind is occasional and may be ignored as far as long-term creep is concerned. In a coordinate system normal and parallel to the slope, the stresses at $Z \leq H_w$ are

$$\tau = [q_o + \gamma H_u + (H_w - Z)\gamma_s] \sin\beta \cos\beta \quad \ldots\ldots\ldots\ldots\ldots\ldots\ldots\ldots \quad (19)$$

$$\sigma = [q_o + \gamma H_u + (H_w - Z)\gamma_s] \cos^2\beta \quad \ldots\ldots\ldots\ldots\ldots\ldots\ldots\ldots \quad (20)$$

The effective stress is

$$\sigma' = \sigma - (H_w - Z)\gamma_w \cos^2\beta \quad \ldots\ldots\ldots\ldots\ldots\ldots\ldots\ldots\ldots\ldots \quad (21)$$

The shear stress has been written, in Eq. 9, in terms of the normal stress $(\sigma_i + \sigma_\gamma + \sigma')$ and $\theta \leq \phi$. Equating this shear to the equilibrium expression in Eq. 19 and using Eqs. 20 and 21 to describe the effective stress, then

$$\tan\theta = \frac{[q_o + \gamma H_u + (H_w - Z)\gamma_s] \sin\beta \cos\beta}{\sigma_i + \sigma_\gamma + [q_o + \gamma H_u + (H_w - Z)(\gamma_s - \gamma_w)] \cos^2\beta} \quad \ldots\ldots\ldots \quad (22)$$

A similar analysis for $Z > H_w$ gives

$$\tan\theta = \frac{[q_o + (H - Z)\gamma] \sin\beta \cos\beta}{\sigma_i + \sigma_\gamma + [q_o + (H - Z)\gamma] \cos^2\beta} \quad \ldots\ldots\ldots\ldots\ldots\ldots \quad (23)$$

Differentiation of Eq. 23 with respect to Z gives tan θ as a monotonically decreasing function of Z and a position, $Z = H_o$, exists where $\theta = \theta_o$ of Eqs. 4, 5, 7, and 8. For $Z > H_o$, $\tau < \tau_o$ and the soil is in the rigid phase; for $Z < H_o$, $\tau > \tau_o$ and the soil is in the creep phase. Additionally, a critical height of ground water occurs where $\theta = \theta_o$. This height is $(H_w)_{crit}$ and in Eq. 23 when $H_w = Z = (H_w)_{crit}$ and $H_u = H - (H_w)_{crit}$, then

$$(H_W)_{crit} = H + \frac{q_o}{\gamma} - \frac{(\sigma_i + \sigma_\gamma)\tan\theta_o}{\gamma\cos^2\beta(\tan\beta - \tan\theta_o)} \quad \ldots\ldots (24)$$

When $H_W > (H_W)_{crit}$ and $Z = H_o$

$$\frac{H_o}{H} = g = \frac{[b + f(1-d) + de](1-h) + (d-a)h}{e(1-h) + h} \quad \ldots\ldots (25)$$

and when $H_W \le (H_W)_{crit}$

$$\frac{H_o}{H} = g = 1 + \frac{b}{f} - \frac{ah}{f(1-h)} = \frac{(H_W)_{crit}}{H} \quad \ldots\ldots (26)$$

Here the following dimensionless arrangements have been used:

$$a = \frac{\sigma_i + \sigma_\gamma}{\gamma_W H\cos^2\beta}; \quad b = \frac{q_o}{\gamma_W H}; \quad d = \frac{H_W}{H}; \quad e = \frac{\gamma_s}{\gamma_W};$$

$$f = \frac{\gamma}{\gamma_W}; \quad h = \frac{\tan\theta_o}{\tan\beta} \quad \ldots\ldots (27)$$

For H_W above $(H_W)_{crit}$, the separation level between the creep and rigidity phases, H_o, increases with H_W. For H_W below $(H_W)_{crit}$, the separation level stays at $(H_W)_{crit}$. The special case of $\theta_o = 0$ ensures that the whole depth is in the creep phase, regardless of σ_γ. Another interpretative feature is that when $g \ge 1$ the whole depth is again in the creep phase.

Fig. 5 represents much of the previous analysis graphically. It is now necessary to find the creep rate, V, for the various possible conditions.

Eq. 1*b*, using Eqs. 8 and 9, may be written as

$$\frac{dV}{dZ}\eta = (\sigma_i + \sigma_\gamma + \sigma')\cos\beta(\tan\theta - \tan\theta_o) \quad \ldots\ldots (28)$$

The introduction of the description of $\tan\theta$ into Eq. 22 for $Z \ge H_W$ and σ' as in Eqs. 20 and 21 allows the definite integral of Eq. 28 between 0 and Z to be completed when it is noted that

$$\frac{\sigma_i + \sigma_\gamma + \sigma'}{\eta} = \lambda \quad \ldots\ldots (29)$$

is largely independent of Z (19). Thus

$$\frac{V}{\lambda H\sin\beta} = -h\frac{Z}{H} - \frac{e}{(1-e)}\frac{Z}{H} + \frac{b + f(1-d) + ea}{(1-e)^2}$$

$$\ln\left[1 + \frac{\frac{Z}{H}(1-e)}{a + b + f(1-d) - d(1-e)}\right] \quad \ldots\ldots (30)$$

When $Z = H_o$ in Eq. 30, the surface creep rate is obtained [V_s in Fig. 5(*b*)]. Then

$$\frac{V_s}{\lambda H\sin\beta} = \frac{1}{(1-e)^2}\left\{-g[h(1-e)^2 + e(1-e)] + [b + f(1-d) + ea]\right.$$

$$\left.\ln\left[1 + \frac{g(1-e)}{a + b + f(1-d) - d(1-e)}\right]\right\} \quad \ldots\ldots (31)$$

Eqs. 30 and 31 are only valid for $H_o \le H_W$; in the case of $H_o \ge H_W$, Eq. 23 must be introduced into Eq. 28 and the quadrature completed over the limits, H_W to Z. Then the difference in creep rates between these limits is

$$\frac{\Delta V}{\lambda H\sin\beta} = -\left(\frac{Z}{H} - d\right)(h-1) + \frac{a}{f}\ln\left[\frac{a + b + f\left(1 - \frac{Z}{H}\right)}{a + b + f(1-d)}\right] \quad \ldots\ldots (32)$$

The creep rate at $H_W \le Z \le H_o$ is

$$V(Z) = V(Z = H_W) + \Delta V(Z) \quad \ldots\ldots (33)$$

giving $\frac{V}{\lambda H\sin\beta} = \frac{1}{(1-e)^2}\left\{-d[h(1-e)^2 + e(1-e)] + [b + f(1-d)\right.$

$$\left. + ea]\ln\left[1 + \frac{d(1-e)}{a + b + f(1-d) - d(1-e)}\right]\right\} - \left(\frac{Z}{H} - d\right)(h-1)$$

$$+ \frac{a}{f}\ln\left[\frac{a + b + f\left(1 - \frac{Z}{H}\right)}{a + b + f(1-d)}\right] \quad \ldots\ldots (34)$$

The creep rate at the surface for the case shown in Fig. 5(*a*) for $H_o < H$ is obtained when $Z = H_o$ in Eq. 34:

$$\frac{V_s}{\lambda H\sin\beta} = \frac{1}{(1-e)^2}\left\{(1-e)[g(1-h)(1-e) - d] + [b + f(1-d) + ea]\right.$$

$$\ln\left[1 + \frac{d(1-e)}{a + b + f(1-d) - d(1-e)}\right] + \frac{a}{f}(1-e)^2$$

$$\left.\ln\left[\frac{a + b + f(1-g)}{a + b + f(1-d)}\right]\right\} \quad \ldots\ldots (35)$$

For $H_o \ge H$ [the case shown in Fig. 5(*c*)], $Z = H$ is substituted into Eq. 34; then

$$\frac{V_s}{\lambda H\sin\beta} = \frac{1}{(1-e)^2}\left\{(1-e)[(1-h)(1-e) - d] + [b + f(1-d) + ea]\right.$$

$$\ln\left[1 + \frac{d(1-e)}{a + b + f(1-d) - d(1-e)}\right] + \frac{a}{f}(1-e)^2$$

$$\left.\ln\left[\frac{a + b}{a + b + f(1-d)}\right]\right\} \quad \ldots\ldots (36)$$

The work of Ter-Stepanian (19) has been extended herein by means of Eqs. 32-36 to account for the region $Z \geq H_W$. The three forms of surface creep envisaged in Fig. 5 and presented in Eqs. 31, 35, and 36 depend on the various features associated with vegetation (a, b, and f), the slope geometry, the water level, and the creep limiting angle. Comparison with the work of Ter-Stepanian (19) is only possible for the situation in Fig. 5(b).

Slope Stability

In this section, the instability of the slope associated with the sudden overcoming of the shear capacity is examined. The factor of safety against such instability is defined as the ratio of the shear capacity to the maximum applied shear. Then

$$F = \frac{[a + b + f(1 - d) + d(e - 1)]\, h'}{b + f(1 - d) + ed + j} \quad \ldots\ldots\ldots\ldots\ldots\ldots\ldots\ldots \quad (37)$$

in which the additional dimensionless arrangements are

$$h' = \frac{\tan \phi}{\tan \beta} \quad \ldots\ldots\ldots\ldots\ldots\ldots\ldots\ldots\ldots\ldots\ldots\ldots \quad (38a)$$

and

$$j = \frac{T_s}{\gamma_w H \sin \beta \cos \beta} \quad \ldots\ldots\ldots\ldots\ldots\ldots\ldots\ldots\ldots\ldots \quad (38b)$$

Sudden slope failure is frequently observed at times of heavy rainfall (2,5,7,8,15). The worst case will be when $H_W = H$. Then

$$F = \frac{(a + b + e - 1)\, h'}{b + e + j} \quad \ldots\ldots\ldots\ldots\ldots\ldots\ldots\ldots\ldots\ldots\ldots\ldots \quad (39)$$

For the infinite slope the maximum applied shear occurs at $Z = 0$. The shear due to the tree overburden and wind are constant through H and the shear associated with the slope mass increases with depth.

Dimensionless Groups

The six dimensionless groups in Eqs. 27 and the two in Eqs. 38 represent the crucial features of the slopes considered. In particular the four factors enumerated by Gray (10) as being of significance in deforestation are: (1) a in Eqs. 27 accounts for the root reinforcement of the soil; (2) b in Eqs. 27 accounts for the vertical slope surcharge; (3) j in Eq. 38b accounts for the wind in the trees; and (4) d and f in Eqs. 27 account for the water level and the soil moisture state. Additionally, physical properties of the soil are exhibited in e and h of Eqs. 27 and h' of Eq. 38a. The geometry of the slope is contained in the normalizing quantities, H and β.

Limiting values and bounds on the dimensionless groups can be obtained from physical and logical arguments. Considerations of geometry suggest $H \geq 5$ ft (1.5 m) and $10° \leq \beta \leq 50°$. A change in creep rate from positive to negative occurs as θ_o passes through the value of β. This means that creep will not occur unless $\beta > \theta_o$ and limits $h < 1$. Values of saturated unit weight vary from

100 pcf (1,600 kg/m^3) for soft slightly organic clays to 130 pcf (2,100 kg/m^3) for stiff hard clays; the cohesion range is from 250 psf (1,200 kg/m^2)-2,000 psf (9,800 kg/m^2) for the same clays. Angles ϕ ranges from 20°-30° for clays of interest; the ratio of creep and ultimate shear stress has been studied (17) and the bounds given of $0.3 < \tau_o/\tau_u < 0.8$ allow h' to be specified. The work of Endo and Tsurata (6) is the only direct measurement of root tenacity. This augmentation of the cohesion depends on the root weight per unit volume and varies from 40 psf (200 kg/m^2)-250 psf (1,200 kg/m^2). The change of σ_γ depends on the value of ϕ for the soil.

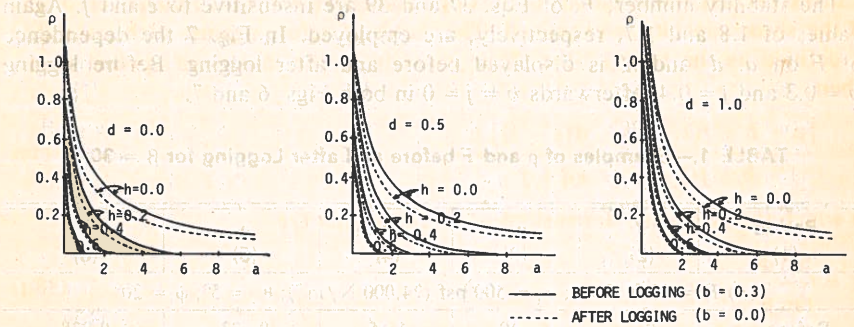

FIG. 6.—Creep ($a - h - \rho$) Curves

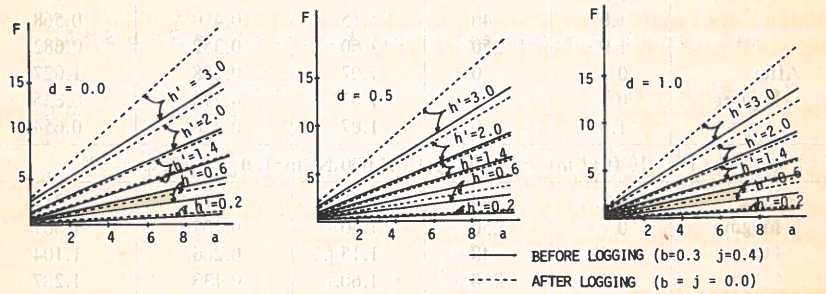

FIG. 7.—Stability ($a - h' - F$) Curves

Superimposed loads due to forests may typically be 50 psf (2,400 N/m^2) (2). Values of 100 psf (4,800 N/m^2) may occur rarely. Davenport (4) has given earth boundary layer constants for forested regions of H_G = 1,200 ft (370 m), $\alpha = 0.2225$, and V_g = 100 mph (160 km/hr). An acceptable drag coefficient is unity with 40 ft (12-m) high trees spaced at 10-ft (3-m) centers and with a continuous profile to the ground. Thus, $C_D = 1$, H_T = 40 ft (12 m), $B(Z) = S$ = 10 ft (3 m).

The dimensionless groups in Eqs. 27 and 38 can now be evaluated as: $0.1 \leq a \leq 16$; $0 \leq b \leq 0.3$; $0 \leq d \leq 1$; $1.6 \leq e \leq 2$; $1.4 \leq f \leq 2$; $0.1 \leq h \leq 1$; $0.4 \leq h' \leq 4$; and $0 \leq j \leq 0.4$.

Interest is concentrated first on the creep rate. Before logging b has a maximum value of 0.3 which decreases to zero after clearing the felled timbers. The

saturated and dry unit weights of soil are tightly bounded and the creep rate proves to be insensitive to the values of e and f. Thus, typical ratios for $e = 1.8$ and $f = 1.7$ are employed in the graphs shown in Fig. 6. Fig. 6 also shows the dependence of the normalized creep rate

$$\rho = \frac{V_s}{\lambda H \sin \beta} \quad \ldots \ldots \ldots \ldots \ldots \ldots \ldots \ldots \ldots \ldots \ldots \ldots \ldots \ldots \quad (40)$$

on the ground-water level, d, soil tension capacity, a, and the creep angle, h. This figure reflects Eqs. 31, 35, and 36.

The stability number, F, of Eqs. 37 and 39 are insensitive to e and f. Again values of 1.8 and 1.7, respectively, are employed. In Fig. 7 the dependence of F on a, d, and h' is displayed before and after logging. Before logging $b = 0.3$ and $j = 0.4$, afterwards $b = j = 0$ in both Figs. 6 and 7.

TABLE 1.—Examples of ρ and F before and after Logging for $\beta = 30°$

Period (1)	d (2)	σ_γ (3)	a (4)	ρ (5)	F (6)
(a) $H = 10$ ft (3 m); $\sigma_i = 500$ psf (24,000 N/m^2); $\theta_o = 5°$; $\phi = 20°$					
Before logging	0	40	1.15	0.323	0.828
	0	250	1.60	0.247	0.946
	0.5	40	1.15	0.354	0.674
	0.5	250	1.60	0.270	0.696
	1.0	40	1.15	0.470	0.568
	1.0	250	1.60	0.352	0.682
After logging	0	0	1.07	0.258	1.027
	0.5	0	1.07	0.293	0.835
	1.0	0	1.07	0.426	0.654
(b) $H = 10$ ft (3 m); $\sigma_i = 500$ psf (24,000 N/m^2); $\theta_o = 10°$; $\phi = 30°$					
Before logging	0	40	1.15	0.175	1.314
	0	250	1.60	0.109	1.501
	0.5	40	1.15	0.206	1.104
	0.5	250	1.60	0.133	1.287
	1.0	40	1.15	0.321	0.902
	1.0	250	1.60	0.211	1.081
After logging	0	0	1.07	0.133	1.629
	0.5	0	1.07	0.168	1.325
	1.0	0	1.07	0.296	1.038
(c) $H = 10$ ft (3 m); $\sigma_i = 500$ psf (24,000 N/m^2); $\theta_o = 15°$; $\phi = 30°$					
Before logging	0	40	1.15	0.056	1.314
	0	250	1.60	0.017	1.501
	0.5	40	1.15	0.087	1.104
	0.5	250	1.60	0.040	1.287
	1.0	40	1.15	0.190	0.902
	1.0	250	1.60	0.099	1.081
After logging	0	0	1.07	0.038	1.629
	0.5	0	1.07	0.073	1.325
	1.0	0	1.07	0.181	1.038

Examples

The use of the graphs in Figs. 6 and 7 are illustrated in Table 1 for an embankment where $\beta = 30°$; $H = 10$ ft (3 m); $\sigma_i = 500$ psf (24,000 N/m^2); and for the following values of θ_o and ϕ: 5° and 20°, 10° and 30°, and 15° and 30°. The values of d considered are 0, 0.5, and 1.0; two values of σ_γ [40 psf (2,000 N/m^2) and 250 psf (12,000 N/m^2)] are used as suggested by Ref. 6. The table then provides the creep rate, ρ, and stability value, F, before and after logging. Tables 2 and 3 illustrate an embankment where $H = 10$ ft (3 m); $\theta_o = 10°$; $\phi = 30°$; $\sigma_i = 500$ psf (24,000 N/m^2); $\sigma_\gamma = 40$ psf (2,000 N/m^2) and 250 psf (12,000 N/m^2); and $d = 0$, 0.5, and 1.0. Values of $\beta = 20°$ are used in Table 2 and $\beta = 40°$ in Table 3.

TABLE 2.—Examples of ρ and F before and after Logging[a] for $\beta = 20°$

Period (1)	d (2)	σ_γ (3)	a (4)	ρ (5)	F (6)
Before logging	0	40	0.98	0.068	1.970
	0	250	1.36	0.025	2.222
	0.5	40	0.98	0.103	1.638
	0.5	250	1.36	0.052	1.885
	1.0	40	0.98	0.227	1.320
	1.0	250	1.36	0.128	1.562
After logging	0	0	0.91	0.047	2.433
	0.5	0	0.91	0.087	1.956
	1.0	0	0.91	0.222	1.505

[a] $H = 10$ ft (3 m); $\sigma_i = 500$ psf (24,000 N/m^2); $\theta_o = 10°$; $\phi = 30°$.

TABLE 3.—Examples of ρ and F before and after Logging[a] for $\beta = 40°$

Period (1)	d (2)	σ_γ (3)	a (4)	ρ (5)	F (6)
Before logging	0	40	1.47	0.208	0.996
	0	250	2.05	0.139	1.161
	0.5	40	1.47	0.233	0.850
	0.5	250	2.05	0.158	1.011
	1.0	40	1.47	0.323	0.709
	1.0	250	2.05	0.218	0.867
After logging	0	0	1.37	0.161	1.241
	0.5	0	1.37	0.189	1.028
	1.0	0	1.37	0.287	0.828

[a] $H = 10$ ft (3 m); $\sigma_i = 500$ psf (24,000 N/m^2); $\theta_o = 10°$; $\phi = 30°$.

Analysis

Consideration of the four features raised by Gray (10) can now be completed based on each occurring independently.

Root Amplification of Soil Tenacity: a in Eq. 27.—In Figs. 6 and 7, the increase of the creep rate parameter, ρ, and the decrease of the stability number, F, with the reduction of a is evident. These changes are independent of the logging procedure, i.e., if for any cause the value of a is decreased and the other dimensionless groups held fixed then the changes will occur. The most common causes of the drop in a are logging and forest fire. During the timber growing period a will increase with subsequent decrease in ρ and increase in F.

Vertical Slope Surcharge: b in Eq. 27.—The value of b changes for 0.3 before logging to zero after logging and ground clearing. The effect is to decrease the creep rate, ρ, and to maintain a more secure embankment.

Wind in Trees: j in Eq. 38b.—The wind effect drops to $j = 0$ after cutting. Before logging, a reasonable value is 0.4. The effect on stability for the joint changes, b and j, is to increase F as shown in Fig. 7.

Soil Moisture Content Change: f in Eqs. 27 and Water Level Change: d in Eqs. 27.—The dimensionless group, f, does not change significantly with clear cutting. However, d will usually increase because of the cessation of evapotranspiration. The result is that ρ increases and F decreases.

The combinded effect of these group changes can be ascertained from Figs. 6 and 7 and from Table 1, 2, and 3 by consideration of chronologically ordered events. After logging, j drops to zero and the possible value of F increase. Clearing reduces b to zero; F definitely increases and ρ decreases. The increase of H_W, and thus d, occurs after these events. Such an increase in d reduces the stability, F, and increases the creep rate parameter, ρ. With further time the σ_γ value decreases eventually to zero and a decreases. The extreme results in Tables 1, 2, and 3 record such events and indicate the worst that can happen after clear cutting.

From this analysis, it is evident that the removal of tree surcharge and the effect of wind in the trees immediately improves the performance of a slope after deforestation. The deterioration of the slope response takes time and is due to root decay and the raising of the water surface. The decay of the root system will be considered first. Swanston (18) indicates that the root system decomposes in 4 yr or 5 yr after logging. This suggests a relationship

$$\sigma_\gamma(t) = \frac{\sigma_\gamma(t=0)}{T^2}(T-t)^2 \quad \ldots\ldots\ldots\ldots\ldots\ldots\ldots\ldots\ldots\ldots \quad (41)$$

for the root tensile strength at time t, in which $\sigma_\gamma(t=0)$ is the root system parameter in the forested region at logging ($t = 0$); T = the time for decay after logging; and t = the time after logging. A possible value of T is 5 yr.

Four possible ways are available for estimating the value $\sigma_\gamma(t=0)$ without involving botanical information: (1) From slope stability of the forested region; (2) from the creep of the forested region; (3) from the individual tree overthrow; and (4) from in-situ measurements such as those of Endo and Tsuruta (6).

Considering 1, the stability of a slope is indicated by the value of F in Eq. 37. In a forested region where no apparent slope instabilities exist, then

$$F \geq 1 \quad \ldots\ldots\ldots\ldots\ldots\ldots\ldots\ldots\ldots\ldots\ldots\ldots\ldots\ldots \quad (42)$$

For $t = 0$ in Eq. 41, $\sigma_\gamma(t=0)$ can be bounded from Eqs. 37 and 42 as

$$\sigma_\gamma(t=0)\,\gamma \geq \left\{(q_o + H\gamma_S)\cos\beta + \frac{T_s}{\cos\rho}\right\}\cot\theta_u - \sigma_i$$

$$+ \gamma_W H\cos\beta - (q_o + H\gamma_S)\cos^2\beta \quad \ldots\ldots\ldots\ldots\ldots\ldots\ldots\ldots \quad (43)$$

The second way of determining $\sigma_\gamma(t=0)\gamma$ is to measure V_S in the forested region and use Eqs. 31, 35, and 36 to compute the value of γ.

The third possible method of evaluating $\sigma_\gamma(t=0)$ requires the consideration of the incipient or complete overthrow of an individual tree. The overturning moment is $M_S\,S^2$ and initially the slipped surface can be considered as the surface of a circular cylinder with radius $r \leq H\cos\beta$ and length S. The shear stress at r is $\bar{\tau}$, in which

$$\bar{\tau} = \frac{M_s S}{\pi r^2} \quad \ldots\ldots\ldots\ldots\ldots\ldots\ldots\ldots\ldots\ldots\ldots\ldots\ldots\ldots \quad (44)$$

Local failure will occur if $\bar{\tau}$ exceeds τ_u in Eq. 8. If $\bar{\tau} \geq \tau_u$ for $Z = H$, then

$$\sigma_\gamma(t=0) \geq \frac{\bar{\tau}}{\tan\phi} - \sigma_i \quad \ldots\ldots\ldots\ldots\ldots\ldots\ldots\ldots\ldots\ldots\ldots\ldots \quad (45)$$

Local disturbance may be detected on the ground ($Z = H$), in which $\sigma' = 0$; and τ_u in Eqs. 8 is a minimum. The value of r can also be included from these ground observations of incipient overthrow. Complete overthrow is associated with the mobilization of τ_u over the slip cylinder. Computations indicate that such overthrow will occur only when the root system is not continuous. This means that failure will occur on an arc outside the root system where the condition is $\sigma_\gamma(t=0) = 0$. This does not help in the determination of the value within the root system.

The incorporation of the previous parameters for S, V_G, H_T, a_T and ϕ into Eq. 45 gives for $r = 10$ ft (3 m)

$$\sigma_\gamma(t=0)\gamma \geq 180 - \sigma_i \quad \ldots\ldots\ldots\ldots\ldots\ldots\ldots\ldots\ldots\ldots\ldots\ldots \quad (46)$$

From inspection of values obtained in the other two approaches used to obtain lower bounds on $\sigma_\gamma(t=0)\gamma$ it is apparent that this last method does not provide better estimates.

Methods 1 and 2 for estimating $\sigma_\gamma(t=0)$ may also be used on a logged slope to determine $\sigma_\gamma(t_1)$ at some time t_1 after logging. The subsequent performance of the slope can then be predicted using the following form of Eq. 41:

$$\sigma_\gamma(t) = \frac{\sigma_\gamma(t_1)}{(T-t_1)^2}(T-t)^2 \quad \ldots\ldots\ldots\ldots\ldots\ldots\ldots\ldots\ldots\ldots \quad (47)$$

Finally, for method 4, when extensive clear cutting is proposed, the original field experiments of Endo and Tsuruta (6) may be repeated. These lead to direct values of σ_i and $\sigma_\gamma(t=0)$ for incorporation in the dimensionless group, a.

The second critical time-dependent change due to logging is the raising of the water table so that d increases. The absence of evapotranspiration after logging causes this increase. Again a time argument such as Eq. 41 is required

to determine d at some time t after logging. Without such evidence a conservative viewpoint suggests $d = 1$ after logging. Figs. 6 and 7 and the tables indicate the severe decrease in F and increase in ρ when d moves from a value smaller than unity before logging to the pessimistic value of $d = 1$ after logging. More realistic evidence of the truly anticipated value of $d(t)$ can produce better and less dismal viewpoints on the creep and stability changes due to logging.

The dimensionless creep rate, ρ, in Eq. 40 contains λ from Eq. 29. Values of σ_i, σ_γ and σ' can be appropriately entered into Eq. 29 from the previous arguments. However, η will increase with the decay of the root system and change of d. Such changes with these soil characteristics do not appear to be documented, but indications are provided by Yen (20).

The arguments in this paper have followed conventional mechanical principles and have paid little heed to the botanical characteristics of the root system. Be this as it may, an essential feature of subsequent work must involve the prediction of $\sigma_\gamma(t = 0)$, $d(t)$, η, b, j, and T by direct examination of the vegetation and its roots. Such predicted values, when included in the analytical schemes of this paper, should provide satisfactory methods of determining the effects of deforestation on slopes.

In the introduction it was noted that Ellison and Coaldrake (5), together with Flaccus (7), were the dissenting authors concerning the effects of deforestation on slope behavior. They stated that logging tended to improve slope stability. Some examination of their views in light of the analyses and conclusions is required herein. The special conditions in southeastern Queensland allow the rapid replacement of the fallen trees by a sod. The roots of the sod are more intense though less thick than those of the fallen trees and extend over the same region and depth of the soil mantle. Thus, instead of $\sigma_\gamma(t)$ being monotonically decreasing with t as in Eq. 47, it appears that $\sigma_\gamma(t)$ would decrease from $\sigma_\gamma(t = 0)$ for a year or so and then increase. The value that it increases to may not be as high as $\sigma_\gamma(t = 0)$, but at the same time, the wind load and tree surcharge cease, and the sod of the region proves to be impermeable and thus the level H_w may be lowered. Such aspects of the Queensland case are evident from Ref. 5. These comments suggest that with d possibly decreasing after clear cutting and $\sigma_\gamma(t)$ only temporarily decreasing, the creep increase and stability deterioration may occur for a only short period of time before a new static equilibrium regime is established. This agrees with the statement by Ellison and Coaldrake (5):

> When trees are felled and burned, and before a sod is established, considerable sliding and rolling takes place so that there is a new adjustment of mantle to slope.

The particular conditions in the rain forest of Queensland may be difficult to replicate in the temperate forest. It is clear that even with the rapid sod growth the slope behavior does deteriorate. However, this is quickly controlled by the establishment of the new root system and lowering of H_w; similar remedial and control procedures may be possible in other climes.

The removal of sod without the ameliorating effects of the reduction in b leads to creep. Thus, in the chalk hills in England the display of White Horses by exposing the white chalk to the required pattern leads to creep of the chalk.

In a century the Hackpen horse crept so that along its back the chalk was 6 in. (150 mm) below the grass, whereas 50 ft (15 m) downhill, at the foot, the chalk was 18 in. (460 mm) above the grass. This evidence again emphasizes, in a different environment from that of Queensland, the importance of a ground cover, other than trees, in controlling motions down a slope.

Flaccus (7) reported his work in the White Mountains where high temperature extremes and intense rainfall exist. The recent glacial area with broken rock cover has slides occurring in times of very intense autumn rainfall. Flaccus indicates that for "theoretical reasons" a mature forest may reduce the slide safety, F. These theoretical reasons must, in light of this paper, be of a botanical nature. In the terms used herein, the roots of trees will always provide values of $\sigma_\gamma(t = 0)$; however, the roots tend to break up the soil and reduce the inherent value of σ_i. Additionally, the high rainfall may maintain d approaching unity before logging. Under these circumstances the relief of the overburden and the absence of wind effects leading to b and j equaling zero appear the dominant features associated with clear cutting. Then ρ decreases and F increases.

The increase of the creep rate with the reduction of the dimensionless group, a, is of greatest important for soils with low cohesion. Soils with high cohesion are largely insensitive to the reduction in $\sigma_\gamma(t = 0)$ and thus the increase in d becomes the most important feature causing the creep rate increase and stability decrease. The change in d will be slower in clay soils than in sandy areas and the adverse manifestation of deforestation on clay slopes takes a long time to become apparent.

Conclusions

The four vegetation features affecting slope behavior (creep and stability) proposed by Gray (10) have been analyzed. It has been found that: (1) The removal of the overburden of trees decreases the creep rate; (2) the cutting and removal of trees with the consequent drop of overburden and wind loading to zero increases the slope stability; (3) the decay of the root system attenuates the soil tenacity especially in soils with low cohesion and increases the creep rate and decreases the stability; and (4) the rising of the water table occasioned by the drop in evapotranspiration increases the creep rate and decreases stability.

Factors 1 and 2 occur immediately after log removal. Factors 3 and 4 take time to become evident. The immediate effect of deforestation is favorable and adverse slope action will only be evident after the presence of (3) and (4) are felt. This suggests ways of maintaining satisfactory slope characteristics after logging by the introduction of ground cover which depresses the water level and provides some root anchorage.

Acknowledgment

Donald H. Gray of the University of Michigan has been generous with his time in examining the deforestation problem. In particular, he drew to the attention of the writers the critical reference by Endo and Tsuruta (6). The funds to support the work were provided by the College of Engineering, University of Washington during the tenure of Dean Emeritus C. H. Norris.

Appendix I.—References

1. Bethlahmy, N., "First Year Effects of Timber Removal on Soil Moisture," International Association of Scientific Hydrology, *Bulletin 7*, No. 2, 1962, pp. 34–38.
2. Bishop, D. M., and Stevens, M. E., "Landslides on Logged Areas in Southeast Alaska," *Forest Service Research Paper NOR-1*, U.S. Department Agriculture, 1964.
3. Croft, A. R., and Adams, J. A., "Landslides and Sedimentation in the North Fork of Ogden River, May 1949," *Research Paper No. 21*, U. S. Forest Service International, Forest and Range Experiment Station, 1950.
4. Davenport, A. G., "Gust Loading Factors," *Journal of the Structural Division*, ASCE, Vol. 93, No. ST3, Proc. Paper 5255, June, 1967, pp. 11–36.
5. Ellison, L., and Coaldrake, J. E., "Soil-Mantle Movement in Relation to Forest Clearing in Southeastern Queensland," *Ecology*, Vol. 35, 1954, pp. 380–388.
6. Endo, T., and Tsuruta, T., "On the Effect of Tree's Roots upon the Shearing Strength of Soil," Annual Report of the Hokkaido Branch Forest Experiment Station, Sapporo, Japan, 1968.
7. Flaccus, E., "Landslides and Their Revegetation in the White Mountains of New Hampshire," thesis presented to Duke University, at Durham, N.C., in 1959, in partial fulfillment of the requirements for the degree of Doctor of Philosophy.
8. Fredriksen, R. L., "Erosion and Sedimentation Following Road Construction and Timber Harvest on Unstable Soil in Three Small Western Oregon Watersheds," *Forest Service Research Paper PNW-104*, U. S. Department Agriculture, 1970.
9. Gaiser, R. N., "Root Channels and Roots in Forested Soils," *Proceedings*, Soil Science Society of America, Vol. 16, 1952, pp. 62–65.
10. Gray, D. H., "Effects of Forest Clear-Cutting on the Stability of Natural Slopes," *Bulletin of the Association of Engineering Geologists*, Vol. VII, Nos. 1 and 2, 1970, pp. 45–66.
11. Heyward, F., "The Root System of Longleaf Pine on the Deep Sands of Western Florida," *Ecology*, Vol. 14, 1933, p. 136.
12. Holch, A. E., "Development of Roots and Shoots of Certain Deciduous Tree Seedlings in Different Forest Sites," *Ecology*, Vol. 12, 1931, p. 259.
13. Hoover, M. D., "Soil Moisture Under a Young Loblolly Pine Plantation," *Proceedings*, Soil Science Society of America, Vol. 17, 1953, pp. 147–150.
14. Jaeger, J. C., *Elasticity, Fracture and Flow*, Methuen, London, England, 1956, p. 105.
15. Kawaguchi, T., Namba, S., and Takiguchi, K., "Landslides and Soil Losses at the Mountain Districts of Izu Peninsula in the Flood of 1958 and Their Control," *Bulletin 117*, Japanese Forest Experiment Station, Tokyo, Japan, 1959, pp. 83–120.
16. McQuilkin, W. E., "Root Development of Pitch Pine, with Some Comparative Observations on Shortleaf Pine," *Journal of Agricultural Research*, Vol. 51, 1935, p. 983.
17. Peck, R. B., Hanson, W. E., and Thornbum, T., *Foundation Engineering*, John Wiley and Sons, Inc., New York, N.Y., 1953, p. 93.
18. Swanston, D. N., "Mechanics of Debris Avalanching in Shallow Till Soil of Southeast Alaska," *Forest Service Research Paper PNW-103*, U.S. Department Agriculture, 1970.
19. Ter-Stepanian, G., "On the Long-Term Stability of Slopes," *Publication 52, Norwegian Geotechnical Institute*, Oslo, Norway, 1963, pp. 1–15.
20. Yen, B. C., "Stability of Slopes Undergoing Creep Deformation," *Journal of the Soil Mechanics and Foundations Division*, ASCE, Vol. 95, No. SM4, Proc. Paper 6675, July, 1969, pp. 1075–1096.

Appendix II.—Notation

The following symbols are used in this paper:

a_T = lower limb height above surface;
$B(Z)$ = tree breadth as function of height;

C = mobilized cohesion strength;
C_D = drag coefficient of wind in trees;
C_o = separation cohesion strength τ_o;
C_u = ultimate cohesion strength;
F = instability factor of safety;
F_S = wind force on single tree parallel to slope;
H = vertical thickness of soil mantle;
H_G = separation height between inviscid and viscous flow;
H_o = separation height τ_o;
H_T = tree limb height (lower limb a_T to top);
H_u = $H - H_W$;
H_W = vertical height of ground-water table above bedrock;
k = wind pressure factor;
M_S = bending moment per unit area of slope surface due to wind in trees;
N = coordinate normal to surface;
q_o = vertical tree surcharge on surface;
r = individual tree slip surface radius;
S = tree spacing;
T = time for complete root deterioration ($\sigma_\gamma = 0$);
T_S = shear per unit area of slope surface due to wind in trees;
t = time after logging;
t_1 = specific time after logging;
V = creep speed;
V_G = inviscid wind speed;
V_S = surface creep speed;
V_W = wind speed in boundary layer;
W = wind pressure;
W_p = wind pressure normal to tree on slope;
Z = vertical coordinate;
β = slope angle;
γ = unit weight of soil;
γ_S = saturated unit weight of soil;
γ_W = unit weight of water;
θ = mobilized shear angle;
θ_o = separation shear angle τ_o;
λ = flow coefficient of soil;
η = soil coefficient of viscosity;
σ' = effective normal compression stress in soil;
$\sigma_\gamma(t)$ = root system strength at time t;
$\sigma_\gamma(t = 0)$ = root system strength at $t = 0$;
τ = mobilized shear stress in soil;
τ_o = maximum τ with zero creep (separation value);
τ_u = ultimate shear strength;
$\bar{\tau}$ = mobilized shear at radius r; and
ϕ = ultimate shear angle or effective angle of soil friction.